Journal of
Applied Crystallography
ISSN 0021-8898

J050007–WF5009

Perturbation method of analysis of crystal truncation rod data

I. K. Robinson *et al.*

Synopsis
Please provide a synopsis (of not more than two sentences) to appear in the *Contents* listing of the journal.

Keywords: PACS; crystal truncation rod.

Queries and comments
Please supply or correct as appropriate all **bold underlined** text.

Author index
Authors' names will normally be arranged alphabetically under their family name and this is commonly their last name. Prefixes (van, de *etc.*) will only be taken into account in the alphabetization if they begin with a capital letter. Authors wishing their names to be alphabetized differently should indicate this below. **Author names may appear more than once in this list; it is not necessary to mark this correction on your proofs.**

Robinson, I.K.
Tabuchi, M.
Hisadome, S.
Oga, R.
Takeda, Y.

$\sigma\Sigma$

doi:10.1107/S0021889805000075

Journal of
Applied Crystallography
ISSN 0021-8898

Received 29 October 04
Accepted 4 January 05

Perturbation method of analysis of crystal truncation rod data

I. K. Robinson,[a,b]* M. Tabuchi,[b] S. Hisadome,[c] R. Oga[b] and Y. Takeda[b,d]

[a]Department of Physics, University of Illinois, Urbana, IL 61801, USA, [b]Venture Business Laboratory, EcoTopia Science Institute, Nagoya University, Furo-cho, Chikusa-ku, Nagoya 464-8603, Japan, [c]Department of Materials Science and Engineering, Nagoya University, Furo-cho, Chikusa-ku, Nagoya 464-8603, Japan, and [d]Department of Crystalline Materials Science, Nagoya University, Furo-cho, Chikusa-ku, Nagoya 464-8603, Japan. Correspondence e-mail: ikr@uiuc.edu

A new method of direct inversion of crystal truncation rod (CTR) data is demonstrated for the analysis of layered semiconductor heterostructure materials. This method is based on approximations that are valid when the electron density deviations and lattice strain are small in the regions of the sample close to a well defined surface. The CTR diffraction pattern can then be regarded as a perturbation with respect to that of an ideal surface. The direct inversion method is shown to work for the analysis of a series of InP/GaInAs/InP heterostructures. The ability to recover strain information is demonstrated with a model calculation. The beginning of breakdown of the perturbation approximation is seen and explained in both cases.

1. Introduction

An important application of the surface X-ray diffraction method is to understand composition profiles in semiconductors, sometimes relevant to doping. Important technologies, such as ultra-high-speed electronics, can be constructed around two-dimensional quantum-well structures where mobility is enhanced by the quantum confinement of electrons or holes at an abrupt chemical interface such as a 'delta-doped' monolayer or a 'double-hetero' quantum-well structure buried inside a bulk semiconductor. Advanced growth techniques, such as organometallic vapor phase epitaxy (OMVPE), can achieve abrupt interfaces under favorable circumstances. Compound semiconductor systems are most favorable because the concentration profiles of two (or more) species can be adjusted, for example to cancel out strain effects in a structure while still achieving substantial modulation of the electronic band gap.

Characterization of the resulting concentration profiles can be challenging. Sectional transmission electron microscopy (TEM) is limited by the sample preparation, which can easily disturb the chemical modulation at the level of single monolayers. Secondary ion mass spectrometry (SIMS) is sensitive to submonolayer concentrations but does not have sufficient spatial resolution and is not sensitive to strain. X-ray diffraction is non-invasive and can be sensitive to both the strain and the concentration (electron density) components of such a heterostructure. In recent years, X-ray diffraction has been used extensively to characterize concentration profiles (Tabuchi *et al.*, 2003, 2000; Takeda & Tabuchi, 2002).

The formalism that encompasses X-ray diffraction from the layering of the material into well defined interfaces is called the crystal truncation rod (CTR) (Robinson, 1986). The simplest case of a CTR is for an ideal surface, or abrupt termination of a bulk crystal at a single atomic plane. For the purposes of this paper, a one-dimensional representation is sufficient, but this can be readily generalized to three dimensions. The sum of phased contributions from the layers of the crystal is dominated by the first layer, which fixes the phase of the sum.

$$A_0(Q) = \sum_{j=0}^{\infty} \rho_0 \exp(iQaj) = \rho_0/[1 - \exp(iQa)]. \quad (1)$$

This is the classic equation (Robinson, 1986) for the complex amplitude, $A(Q)$, for a CTR as a function of the total momentum transfer, $Q = 2k \sin\theta$, derived from the Bragg angle, θ, where $k = 2\pi/\lambda$ is the wavevector and λ is the wavelength of the X-rays. The ideal crystal is modeled as a stack of equally spaced layers of density ρ_0 starting at $j = 0$ with lattice spacing a. The intensity of the scattered X-rays is proportional to $|A_0(Q)|^2$, where form factors, geometry factors and fundamental constants have been ignored for simplicity. The phase of the complex amplitude is always lost because the detectors are insensitive to it. Variations of the CTR have been described to account for the effects of variable layer spacing and surface roughness, and a widely used data analysis program, *ROD*, has been developed (Vlieg, 2000). The application of CTRs to study surface structure has been reviewed (Robinson & Tweet, 1992; Feidenhans'l, 1989; Shimura & Harada, 1993; Robinson, 1990).

In this paper, we demonstrate that simple expansions of equation (1) can be used to reveal electron density and strain

profiles inside crystals so long as those perturbations remain small. For studying double heterostructures of composition $In_{1-x}Ga_xP_{1-y}As_y$, the strain and electron density couple in an almost perfect bilinear manner with the composition variables x and y, which allows them to be extracted directly from the CTR data. This will be demonstrated with measurements of an actual sample heterostructure.

2. Perturbation of density by a step

The simplest heterostructure showing a change of electron density in its layering is the 'double step' structure, where there is a single step (increase or decrease) in the crystal density profile at a certain depth below the surface of the sample. The topmost n layers have a density ρ_1, while the remainder of the sample has density $\rho_1 + \rho_2$. The interface at a depth na inside the structure is assumed to be perfectly abrupt. The CTR from the double step can be constructed as a superposition of two CTRs with weights ρ_1 and ρ_2, starting at layers $j = 0$ and $j = n$:

$$\begin{aligned} A_1(Q) &= \sum_{j=0}^{\infty} \rho_1 \exp(iQaj) + \sum_{j=n}^{\infty} \rho_2 \exp(iQaj) \\ &= \left[\rho_1 + \rho_2 \exp(iQan)\right]/[1 - \exp(iQa)] \\ &= M_1(Q)/[1 - \exp(iQa)]. \end{aligned} \tag{2}$$

It can be seen from the factorization of the result that the original CTR amplitude becomes multiplied by a modulation function $M_1(Q) = \rho_1 + \rho_2 \exp(iQan)$. Even though both of these factors are complex, the magnitude of their product is the product of the magnitudes. Therefore, $|M_1(Q)|$ is experimentally observable because the measured intensity function can be divided by the ideal CTR intensity, $|A_0(Q)|^2$, to give a quantity proportional to $|M_1(Q)|^2$.

In general, $|M_1(Q)|^2$ would be no more easy to analyze than (2), but in the perturbation limit $\rho_2 \ll \rho_1$ the situation is considerably simplified because the imaginary part of $M_1(Q)$ can be neglected:

$$\begin{aligned} |M_1(Q)| &= \left|\rho_1 + \rho_2 \exp(iQan)\right| \\ &\simeq \rho_1 + \rho_2 \cos(Qan). \end{aligned} \tag{3}$$

An arbitrary, density modulated, heterostructure can be considered as a superposition of a number of such steps at various layer positions n, in which the perturbation, $\rho_2(n)$, can be positive or negative, so long as it remains small. From the perspective of data analysis, this is a great simplification because $|M_1(Q)|$ can be measured and Fourier transformed to determine the weight (ρ_2) and position (na) of each step in the structure. In this way an arbitrary density profile can be recovered, so long as the lattice parameters of all layers of the structure are identical. The only approximation is the simplest perturbation limit, $\rho_2 \ll \rho_1$: all the internal steps must be small compared with the density step of the surface itself.

3. CTR data analysis protocol

This suggests the following data analysis procedure. The measured $I(Q)$ is divided by the theoretical intensity distribution for an ideally terminated surface, $|A_0(Q)|^2$, defined by equation (1), to give the experimental modulation function,

$$\begin{aligned} M(Q) &= [I(Q)]^{1/2}/|A_0(Q)| \\ &= [I(Q)]^{1/2} \sin(Qa/2). \end{aligned} \tag{4}$$

The experimental $M(Q)$ is then Fourier transformed. The transform will consist of a symmetric set of δ-functions, broadened by the cut-off resolution of the data. The largest peak in the transform will be the origin peak with an amplitude of ρ_1, while all other density steps will produce small peaks of amplitude ρ_2, which can be positive or negative. Given that a δ-function is the spatial derivative of a step, we can then synthesize the density profile of the sample by integration:

$$\rho(z) = \int_0^z \mathcal{F}\{[I(Q)]^{1/2} \sin(Qa/2)\}\, dz'. \tag{5}$$

If the momentum transfer Q were retained directly from the data, the resulting image of the crystal from (5) would show the changes of density modulating the crystal lattice, which is a rapidly oscillating function. It is more informative to view just the density profile as the envelope of the lattice function. This is obtained in a straightforward way by expressing the data as a function of the *reduced* momentum transfer, $q = Q - Q_0$, where Q_0 is the position of the Bragg peak. The data will then be distributed around the origin of q and contain only low-frequency components, whose transform is the slow-varying density envelope function.

This method is a close analog of the 'master equation' of Als-Nielsen (Als-Nielsen, 1985; Als-Nielsen & McMorrow, 2000), widely used to analyze X-ray reflectivity. The measured reflectivity is first divided by the Fresnel reflectivity, then Fourier transformed and integrated to obtain the profile. The formal derivation involves integration-by-parts of the equation relating the reflectivity to the density profile (Als-Nielsen & McMorrow, 2000). In practice, the integration step, equation (5), can often be omitted because the sharpness of each interface can be more readily determined by direct inspection of $\mathcal{F}\{|M(Q)|\}$.

4. Perturbation by strain

The case of a strained crystal can be handled in an analogous way. Here the elementary case to be considered is to introduce a local perpendicular displacement, u, into the sequence of layers in the nth layer, with all layers having the same density, ρ_0. All subsequent layers are then shifted by the distance u, so the CTR amplitude has to be written as the sum of two sequences with an offset

$$A_2(Q) = \sum_{j=0}^{n-1} \rho_0 \exp(iQaj) + \exp(iQu) \sum_{j=n}^{\infty} \rho_0 \exp(iQaj)$$
$$= \rho_0 \left[\frac{1 - \exp(iQan)}{1 - \exp(iQa)} + \exp(iQu) \frac{\exp(iQan)}{1 - \exp(iQa)} \right]$$
$$= \{\rho_0/[1 - \exp(iQa)]\}\{1 + \exp(iQan)[\exp(iQu) - 1]\}. \quad (6)$$

The perturbation approximation is that the displacement is small, $Qu \ll 1$, so that $\exp(iQu) - 1 \simeq iQ_0u$. An additional approximation of assuming a small range of momentum transfer around a Bragg peak $Q \simeq Q_0$ has been made. Once again the result factorizes into an ideal CTR and a modulation function,

$$A_2(Q) \simeq \left[\rho_0 + iQ_0u\rho_0 \exp(iQan)\right]/[1 - \exp(iQa)]$$
$$= M_2(Q)/[1 - \exp(iQa)]. \quad (7)$$

In the same small displacement limit, the magnitude of the modulation function can be approximated as its real part,

$$|M_2(Q)| = \left|\rho_0 + iQ_0u\rho_0 \exp(iQan)\right|$$
$$\simeq \rho_0 - Q_0u\rho_0 \sin(Qan). \quad (8)$$

As is customary, there is no effect of strain for $Q_0 = 0$ and the coupling becomes stronger at larger Q_0. This time, the Q-dependent part of the modulation is an antisymmetric function around the $Q_0 \neq 0$ Bragg peaks. The Fourier components will be *imaginary* δ-functions located at positions $\pm na$. The general case of a strain distribution, so long as the strain is not too large, will be reproduced in the imaginary part of the Fourier transform of the measured $M(Q)$. (See §7.)

Combining the two parts, we have a general method for extracting density and strain profiles from the data in the perturbation limit.

(i) Divide $[I(Q)]^{1/2}$ by an ideal CTR amplitude.
(ii) Fourier transform the resulting $M(Q)$.
(iii) $\Re\{\mathcal{FT}\}$ is the density derivative profile.
(iv) $\Im\{\mathcal{FT}\}$ is the strain profile.

5. Sample preparation and measurements

The samples were grown by OMVPE using triethylgallium, trimethylindium, tertiarybutylarsine and tertiarybutylphosphine precursors in a hydrogen carrier gas at 76 Torr. The compositions were determined to lattice match the two materials as closely as possible. A pure InP buffer layer of 100 nm was grown at 293 K on an InP substrate, followed by a variable number of layers with composition $Ga_{0.47}In_{0.53}As$, optimized to have the same lattice parameter as *InP*. Finally, a capping layer of 45 monolayers (ML) of InP was grown on top. The objective was to create interfaces that are as abrupt as possible (Tabuchi *et al.*, 2004).

The CTR intensity measurements were made at BL18B of the Photon Factory, Tsukuba, Japan (Tabuchi *et al.*, 2000). A wavelength of 1.6 Å was selected using a Si(111) double-crystal monochromator. The Weissenberg geometry was used to record the CTR on each side of the Bragg peak on a charge-couple device (CCD) detector. Integration of the CTR intensity was achieved by rocking the sample during the measurement, taking care not to pass through the InP Bragg peak (Robinson, 1990). The integrated intensity was extracted from the CCD by using numerical integration along perpendicular lines to estimate the background.

Data were only measured around the (002) reflection. This was chosen because the contrast between InP and GaInAs is very strong; InP has a fairly large structure factor, while GaInAs is about five times weaker. The validity of the perturbation approximation is questionable in this case. Nevertheless, these were better samples to consider than those based on GaAs substrates for which the (002) structure factor is rather small. The absence of strain allows us to test the direct inversion method in its simplest form. This point is discussed further below.

6. Results for density profiles

The measured CTR intensity profiles were analyzed directly using equation (5). Since the samples were designed to be free of strain, the amplitude-only version of the analysis could be implemented, as described in §§2 and 3. A computer program was written to evaluate the expression in equation (5). The program employed a fast Fourier transform (FFT) to transform data arrays of size N = 2048 (Press *et al.*, 1992). This procedure allows sufficient zero-padding of the ~800 data points to avoid aliasing. The measured data were equally spaced with an increment of momentum transfer of $\Delta L = 0.00088$ (typical) reciprocal lattice units (RLU), so that these could be packed into adjacent elements of the FFT input array, with the origin shifted to the Bragg peak position. Each data set had a different value of ΔL. The spacing of array points in the output array, Δn, measured in atomic layers can then be obtained by equating the momentum transfer, $Q = (2\pi/a_0)L$, the layer spacing (which is half the lattice parameter), $a = a_0/2$, and the physical position in the layered structure, $z = na$, by the definition of the phase factor in the FFT,

$$\exp(iQz) = \exp[i(j\Delta Q)(k\Delta z)] = \exp\{i[j(2\pi/a_0)\Delta L](ka\Delta n)\}$$
$$= \exp(2\pi ijk/N)$$
$$\Rightarrow \Delta n = 2/N\Delta L = 1.11 \text{ layers}. \quad (9)$$

In equation (9), the symbols j and k are just the index variables that span the arrays that are connected by the FFT. If finer-spaced points are required in the real-space profile, a larger FFT dimension, N, can be employed. Once this program was implemented, several problems were immediately detected that led to revisions of the analysis method to take account of the limitations of the real data.

Firstly, the center of the CTR was not measured because of the presence of the Bragg peak that would saturate the detector. It has previously been shown (Robinson & Tweet, 1992; Feidenhans'l, 1989; Shimura & Harada, 1993; Robinson, 1990; Als-Nielsen, 1985; Als-Nielsen & McMorrow, 2000; Tabuchi *et al.*, 2004; Press *et al.*, 1992; Afanasev *et al.*, 1989) that the measurements are asymptotic to the ideal form of the CTR. Real measurements close to the peak can be very hard

to make because of detector imperfections, mosaicity, finite resolution *etc*, and ultimately are limited by dynamical diffraction at the Bragg point itself (Afanasev *et al.*, 1989). Thus it will always be the case that there is a gap in the center of the data. Once the data have been divided by the CTR as in equation (4), the amplitude should be just constant very close to the center. For this reason the data used for our calculations were 'bridged' by a constant value equal to the average of the last data point on the two sides.

Secondly, the data end abruptly at a cutoff value where the intensity of the measurement is considered to have reached the noise level. After application of equation (5), this leads to a non-physical step at the beginning and end of the scan. The statistics become amplified by equation (5) near the ends of the range where the data also become noise. It is therefore desirable to filter the data at this point by multiplication by a pair of Fermi functions, $f_{\rm FILTER} = 1/\{1 + \exp[(Q - Q_{\rm F})/W]\}$, where the constants for the cut point, $Q_{\rm F}$, and spread, W, are adjusted by visual inspection. Since the abrupt cutoff leads to ripples in the derived density function, the values of $Q_{\rm F}$ and W could be adjusted *post facto* by tuning the suppression of the ripples. The effect of the filter on the appearance of the modulus of the measured transform, $|M(Q)|$, are illustrated in Fig. 1.

The last revision to the method was the most sensitive. The position of the Bragg peak was estimated carefully on the CCD used for recording the CTR, but the procedure is prone to small errors. As can be seen in the experimental curves in Fig. 2, the shapes of the intensity minima are very sharp so the momentum transfer scale must be centered exactly to measure their positions correctly. Any small error will lead to asymmetric data and will appear as strain in the analysis. Initially, it was found that peaks were appearing in the imaginary part of the derived density, $\Im\{\mathcal{F}\{|M(Q)|\}\}$, at the locations of the density steps, as if the transform were 'rotated' in the complex plane. The solution was to adjust the center position of the data manually to minimize these imaginary peaks. For the two-step structure, both peaks were found to disappear with the same shift, suggesting this revision to the procedure was appropriate. All five data sets needed shifting in the same direction, suggesting a systematic origin. The biggest shift needed was 0.007 RLU, which is a reasonable error for the measurement.

Once these precautions were taken, the resulting density profiles could be obtained in a semi-automatic way. The results are plotted for the five samples investigated in Fig. 3. It is pleasing to see the box-like dip in the density at the expected location inside the samples. The position of the step down is about 45 layers in all cases, as designed. The step up is deeper, as expected, and is symmetric with the step down. The sharpness of the step edges is mainly due to resolution of the data cutoff; sharper edges could be produced when the filter, multiplication by $f_{\rm FILTER}$, was turned off, but at a cost of introducing ripples in the profile. The magnitude of the dip is not quite as big as would be expected from the known sample composition, but it agrees fairly well among the samples. The size of the large density step corresponding to the sample

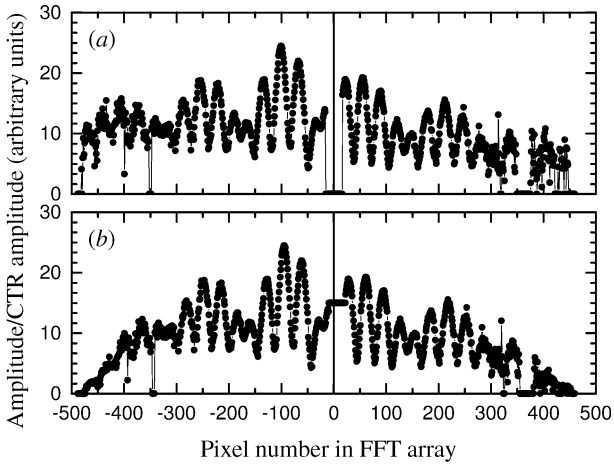

Figure 1
Illustration of the packing of the data points into an array for application of the FFT. (*a*) Raw amplitude data for the 10 ML sample after dividing by the ideal CTR amplitude, according to (4). (*b*) The same after the following treatments: (i) shifting of the center by six points to minimize the imaginary part of the FFT, (ii) filling the center of the array, (iii) filtering the ends by multiplication by Fermi functions of width W = 30 FFT grid points.

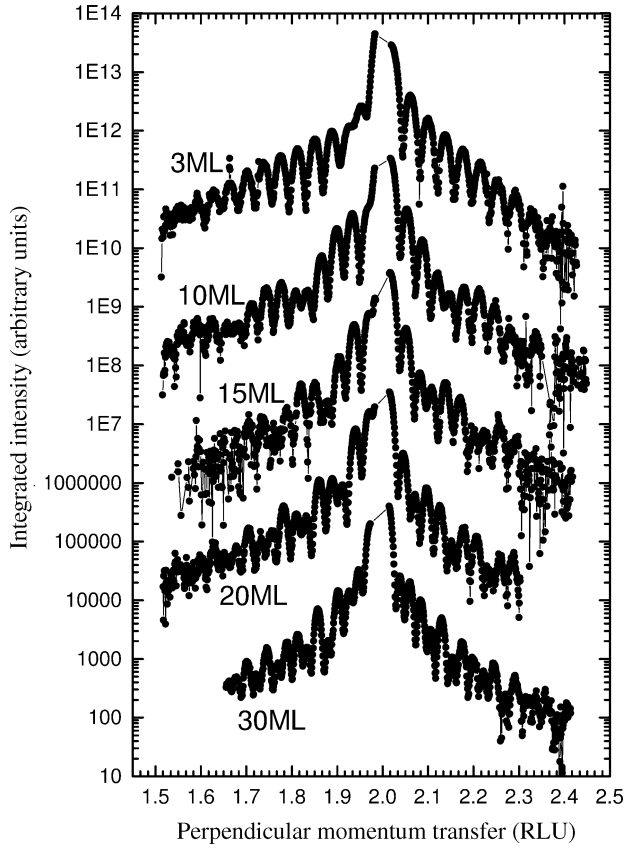

Figure 2
Raw CTR data for the five samples evaluated in this paper, measured for the (00L) CTR around the (002) reflection. The CTR intensity extracted from the CCD has been integrated and background subtracted. The curves have been scaled to match at their centers and then offset by two decades for clarity. The labels indicate the nominal composition as the number of GaInAs layers, followed by 45 monolayers (ML) of InP.

surface is sensitive to the lower bound of the integral in equation (5). The zeroth element of the FFT is given by the sum of all the data magnitudes in the input array and so is sensitive to the scaling of the data. For this reason, the integral plotted in Fig. 3 is the sum of the real part of the derivative density array, corresponding to $\Re\{\mathcal{F}\{|M(Q)|\}\}$, starting at array element number one and ending at the depth indicated.

There is a smooth curved variation of density underlying the sharp features that are the desired image of the heterostructure density; these can be attributed to the imperfect filling of the center of the diffraction pattern under the Bragg peak, mentioned above. More troubling is the extra step that occurs in all the density profiles, lying between the surface and the box-shaped dip of the GaInAs heterostructure, which is unexpected. Closer inspection reveals that the position of the spurious step is equal to the thickness of the GaInAs heterolayers, which strongly suggests it is an artefact. Simulations of calculated CTR profiles showed the same thing, but only for a double-step structure and with a non-linear dependence on the size of the perturbation density step, ρ_2 in equation (2); when $\rho_2 \ll \rho_1$ the artefact did not appear, but it grew rapidly in size until it was almost equal to the object step itself when $\rho_2 \simeq \rho_1$.

The fact that the spurious step occurs at a difference frequency in the Fourier transform and the nonlinear dependence on the magnitude of ρ_2 suggest that it is due to a breakdown of the perturbation approximation. The expansion of the modulation function in equation (3) can be re-evaluated for the case of equal down and up density steps of $\mp\rho_2$, at positions $z = n_1 a$ and $n_2 a$, respectively, retaining the higher-order terms, which arise from the imaginary parts of the complex exponentials combining together in the magnitude of the modulation function,

$$\begin{aligned} |M_3(Q)| &= \left|\rho_0 + \rho_2\left[\exp(iQan_2) - \exp(iQan_1)\right]\right| \\ &\simeq \rho_0 + \rho_2\left[\cos(Qan_2) - \cos(Qan_1)\right] \\ &\quad - (\rho_2^2/2\rho_1)\cos[Qa(n_1 - n_2)]. \end{aligned} \tag{10}$$

There are also some extra terms at **sum [some?]** frequencies, which have been omitted. It is seen from the ρ^2 dependence that this last term is second order in the density perturbation and that it becomes important only when $\rho_2 \simeq \rho_1$. Unfortunately, that is the case for our heterostructures of GaInAs inside InP measured at the (002) reflection. Considering just the $Q = 0$ form factors, the (002) structure factor for InP is $\rho_1 = 34e$, while that of GaInAs is only $7e$, so $\rho_2 = 27e$. According to equation (10), the real steps should be $\pm 27e$ in size, while spurious step should be $10.7e$. This statement agrees roughly with the observation in Fig. 3. The sign of the second-order term is always negative, whatever the sign of ρ_2, and this is also seen in the data.

7. Testing of the method for strain profiles

The series of samples just discussed was chosen specifically to be strain-free. No suitable samples containing strain were available for testing the method of extracting strain profiles as the imaginary part of the Fourier transform of the modulation function, as discussed in §4 above. We therefore explore this capability with a test calculation, which simulates what could be obtained experimentally.

The CTR intensity data were simulated with the program *ROD*, which is widely assumed to be reliable for this purpose (Vlieg, 2000). A model heterostructure was composed of layers of Si atoms, with an increased layer spacing $\Delta d/d$ over 20 layers, followed by a 'cap' of 26 more Si layers with the bulk spacing. The intensities of 400 equally spaced data points were calculated over the range $1.6 < L < 2.4$, around the 002 reflection, assuming a primitive structure with two layers per unit cell.

These simulated data were treated in the same way as described in §6, dividing by an ideal CTR profile to extract the modulation function, filtering and finally taking the Fourier transform. The imaginary parts were then plotted directly in Fig. 4 as a function of the depth, given by the layer number, n, defined in equation (9). The density profile (not shown) was obtained by integration of the real parts, according to equation (5), but it had no features other than a large step at the origin and a few ripples.

Fig. 4(a) shows the effect of varying the filter-width parameter, W, to illustrate that the data-filtering step is important, as was found for the real data. Undesirable ripples appear in the profile if the data are cut off too abruptly; when too much filtering is employed, the profile becomes too rounded and softened in amplitude. A good compromise appears to be

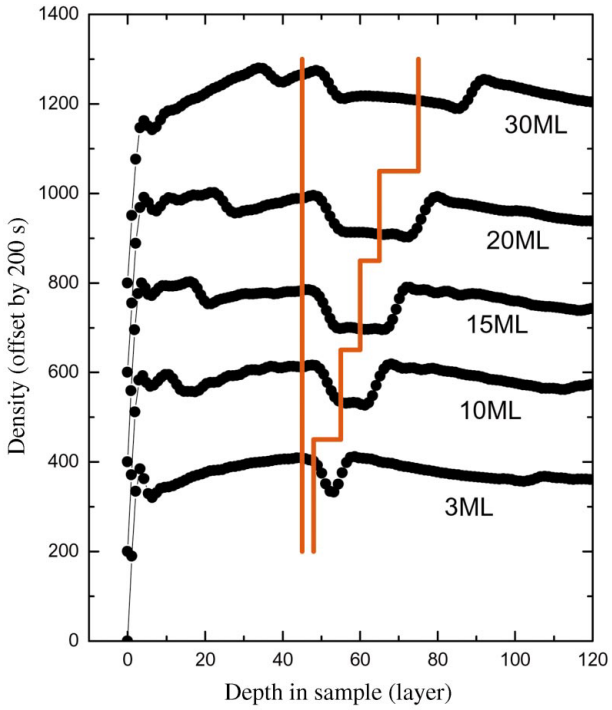

Figure 3
Derived density profiles for the five samples investigated. The nominal composition was the number of GaInAs layers indicated by the label on each curve, followed by 45 monolayers (ML) of InP. The curves are offset by 200 units on the vertical scale. The expected positions of the steps in the profiles are also indicated by (red) vertical lines.

$W = 30$, which was then used for the subsequent tests. Note that there is also a small ripple appearing near the origin, $n = 0$.

Fig. 4(b) shows the response to varying the amount of strain in the model heterostructure. A roughly linear trend is found for the first two tests, up to $\Delta d/d = 0.5\%$, but the third profile, with $\Delta d/d = 0.75\%$, is badly distorted on its trailing edge. Other distortions in the flat regions outside the strained region are also seen to be emerging. This behavior appears to define the limit where the perturbation approximation is starting to break down. The accumulated strain over the 20-layer slab means that the whole cap layer is displaced outwards by $u = 0.15a$, where a is the layer spacing. Thus $Q_0 u = 0.15 \times 2\pi = 0.94 \simeq 1$ as predicted above for the breakdown. The reason why the strain profile becomes distorted asymmetrically on its lower edge is not understood at this time.

8. Conclusions and outlook

The basic result that density profiles can be extracted from CTR data by direct inversion is highly encouraging. Meaningful profiles were obtained for all five samples investigated.

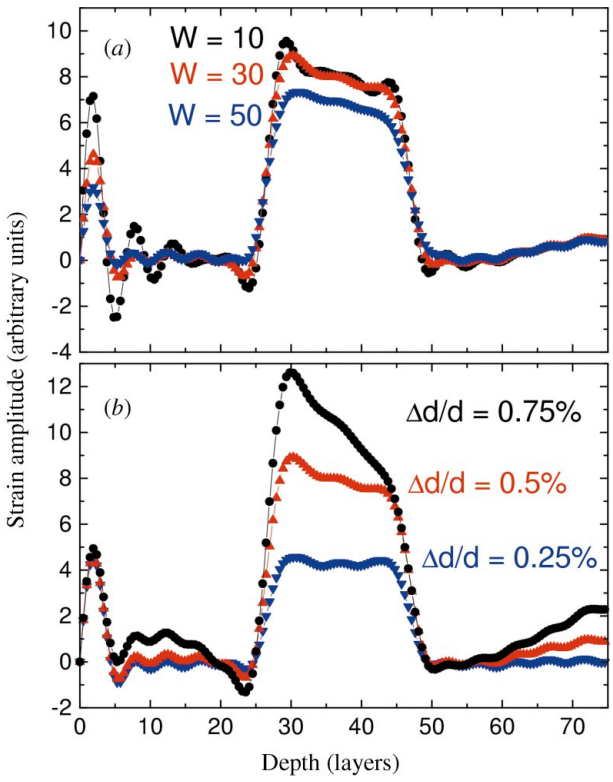

Figure 4
Strain profiles derived from test calculations for a buried slab of 20 layers of strained material with constant density buried under a cap of 26 layers. Plotted on the vertical axis is the imaginary part of the Fourier transform of the modulation function for a variety of test conditions. (a) variation of the filter parameter used to smooth the cutoff at the end of the data range, W, measured in grid points of the N = 2048 FFT employed. (b) Variation of the response to different amounts of strain, $\Delta d/d$, within the 20-layer slab, showing the onset of distortions.

No iteration is involved, but some adjustment of filters and centering is found to be important to obtain the right result. The method can, in principle, be extended to strained samples, where the strain profile appears in the imaginary part of the transform, but this process will need more care because the appearance of an imaginary part is also caused by small miscenterings of the data. One artefact, a spurious extra step, was found in all cases and explained as a breakdown of the perturbation approximation. The size and sign of the artefact agrees with estimates of the second-order term in the expansion.

One discrepancy that has become apparent is the disagreement in Fig. 3 between the derived and expected positions of the density steps in the profile. All five samples have the step down in the same place, but it is nearer to 51 ML deep than the 45 ML designed. The up steps appear lower in the sample by 5, 13,18, 24 and 37 ML rather than the 3, 10, 15, 20 and 30 ML planned. This result might be explained by miscalibration of the growth rates by about 14% for InP and 23% for GaInAs. The positions in Fig. 3 agree very well with those obtained by fitting the CTR profiles (Tabuchi *et al.*, 2004), particularly for the As composition profile, consistent with the idea of growth rate miscalibration. The calibration of the horizontal axis of Fig. 3 comes directly from equation (9) and is different for each set of measurements because of their different values of ΔL. Other conceivable sources of error lie with the measurements in the calibration of wavelength, CCD readout and detector distance.

The sharpness of steps is a relevant technological problem, and the desired quantum confinement effects are strongest at an abrupt chemical interface; any smearing implies disorder, which causes scattering of the electrons and hence lower mobilities. Single-sided exponential functions were used in the fitting of the profiles because that is an appropriate model for diffusion of a single species (Tabuchi *et al.*, 2004). In our model-independent profiles, **the profiles are seen to be more symmetric**. However, the steepness of the steps was found to change with the degree of filtering of the data, so this is apparently a resolution effect. In principle, the resolution (measured range) of the data determines how sharp a feature can be detected, but features can be identified by fitting beyond the nominal resolution. However, ambiguities may result.

For the samples used in these studies, the artefact step was well separated from the features of interest in the heterostructure. The observed breakdown of the perturbation approximation was not a problem, except that the sizes of the real steps in the density profile were underestimated because of the inherent nonlinearities of the higher-order terms. New samples could be designed closer to the perturbation limit to verify the applicability of the formalism. It would also be good too test the ability to detect strain by this method. Other directions to be explored in the future include the use of the (004) (or other) reflection, which is strong for GaAs-based samples. The combination of (002) and (004) data might allow more reliable estimates of the amplitude and strain components with a certain degree of redundancy.

This work was partly supported by the NSF under grant DMR 03-08660, and by a Grant-in-Aid for Scientific Research (B) No. 16360006 from the Ministry of Education, Science, Sports and Culture. The experiments at the Photon Factory were performed as part of peer-reviewed projects 2002 G219 and 2003 G218. The collaboration was initiated under the 'VBL invitation program'.

References

Afanasev, A. M., Imamov, R. M., Lomov, A. A. *et. al.* (1989). *Fizika Tverdogo Tela*, **31**, 176–181. **Please give full list of authors if possible.**

Als-Nielsen, J. (1985). *Z. Phys. B Conden. Matter*, **61**, 411–414.

Als-Nielsen, J. & McMorrow, D. (2000). *Elements of Modern X-ray Physics*. **Town, country of publication?**: John Wiley and Sons Ltd.

Feidenhans'l, R. (1989). *Surf. Sci. Rep.* **10**, 105–188.

Press, W. H., Flannery, B. P., Teukolsky, S. A. & Vetterling, W. T. (1992). *Numerical Recipes in C: The Art of Scientific Computing*. Cambridge University Press.

Robinson, I. K. (1986). *Phys. Rev. B*, **33**, 3830–3836.

Robinson, I. K. (1990). *Handbook on Synchrotron Radiation*, Vol. III, edited by D. E. Moncton & G. S. Brown. **Town, country of publication?**: North-Holland/Elsevier.

Robinson, I. K. & Tweet, D. J. (1992). *Rep. Prog. Phys.* **55**, 599–651.

Shimura, T. & Harada, J. (1993). *J. Appl. Cryst.* **26**, 151–158.

Tabuchi, M., Hisadome, S., Yamada, H., Oga, R. & Takeda, Y. (2004). Proceedings of the 2004 International Conference on Indium Phosphide and Related Materials (IPRM 2004), Kagoshima, Japan.

Tabuchi, M., Kyouzu, H., Takemi, M. & Takeda, Y. (2003). *Appl. Surf. Sci.* **216**, 526–531.

Tabuchi, M., Takahashi, R., Araki, M., Hirayama, K., Futakuchi, N., Shimogaki, Y., Nakano, Y. & Takeda, Y. (2000). *Appl. Surf. Sci.* **159–160**, 250–255.

Takeda, Y. & Tabuchi, M. (2002). *J. Cryst. Growth*, **237**, 330–337.

Vlieg, E. (2000). *J. Appl. Cryst.* **33**, 401–405.

INTERNATIONAL UNION OF CRYSTALLOGRAPHY

Electronic Proof Instructions

These proofs should be returned **within 14 days of January 14 2005**. After this period, the Editors reserve the right to publish articles with only the Managing Editor's corrections.

Please

(1) Read these proofs and assess if any corrections are necessary.

(2) Check that any technical editing queries have been answered.

(3) Return any corrections immediately

(a) by e-mail to

ps@iucr.org

giving a full description of the corrections in plain text and indicating the page, column and line numbers where appropriate.

(b) by fax to

+44 1244 314888

If the corrections are too complicated to send by e-mail please mark your corrections on the proofs as indicated overleaf. It is recommended that authors check that the fax transmission has been successful.

(4) Authors are not required to return proofs by mail. However, if you wish to do this please send them to

Mr P. Strickland
Managing Editor,
International Union of Crystallography,
5 Abbey Square,
Chester CH1 2HU,
England

Telephone: +44 1244 342878

Substantial alterations, apart from occasioning delay in publication, are much more expensive than many authors would suppose. Authors may therefore be required to pay for any major alterations from their original copy, and it may sometimes be necessary to disallow such changes. Where alterations are unavoidable every effort should be made to substitute words or phrases equal in length to those deleted.

Please note that in order to save postal expenses and clerical work, the typescript, drawings and photographs of articles are normally destroyed after publication. Drawings and photographs will only be returned to authors if their return is specifically requested.

Authors will be informed by e-mail when their paper is published and may then download an electronic offprint of their paper from the author services page of **Crystallography Journals Online** (**http://journals.iucr.org**)

Printed offprints may be purchased using the attached form which should be returned as soon as possible. It will not be possible to supply offprints for orders received after the journal is printed.

Proof Corrections

If returning your corrections by fax (or mail) please use the marking system below. Please ensure that you use black ink (not pencil) and that you do not make corrections too near the edge of the page as these may be lost in transmission.

Please do not make corrections to the pdf file electronically and please do not return the pdf file.

The recommended system of marking corrections is as follows.

(1) Each place in the text where a correction is needed should be indicated either by crossing out the characters to be corrected or by an insert mark (/) if an insertion is needed.
(2) The correct character, word, instruction or insertion should be shown in the margin at one end of the line and should be terminated with a long slash mark (/).
(3) The corrections in the margins (both left and right margins may be used) should be arranged in the same sequence as they are required in the line of text.
(4) Characters to be printed in the superior position, such as superscripts, apostrophes and quotation marks, are to be so identified by the symbol ∨ under them, e.g. x^2 or x''. Characters to be printed in the inferior position, such as subscripts, are to be identified by the symbol ∧ over them, e.g. A_2.
(5) Instructions written in the margins should be encircled. This indicates that this text is not to be printed. This does not apply to the full stop (period), the colon and the solidus (slash mark), which are circled for clarity.
(6) Some instructions are needed so frequently that it is convenient to indicate them simply with special symbols or abbreviations. The symbols are recognized as instructions without being circled. Some frequently used instructions are given in the following list.

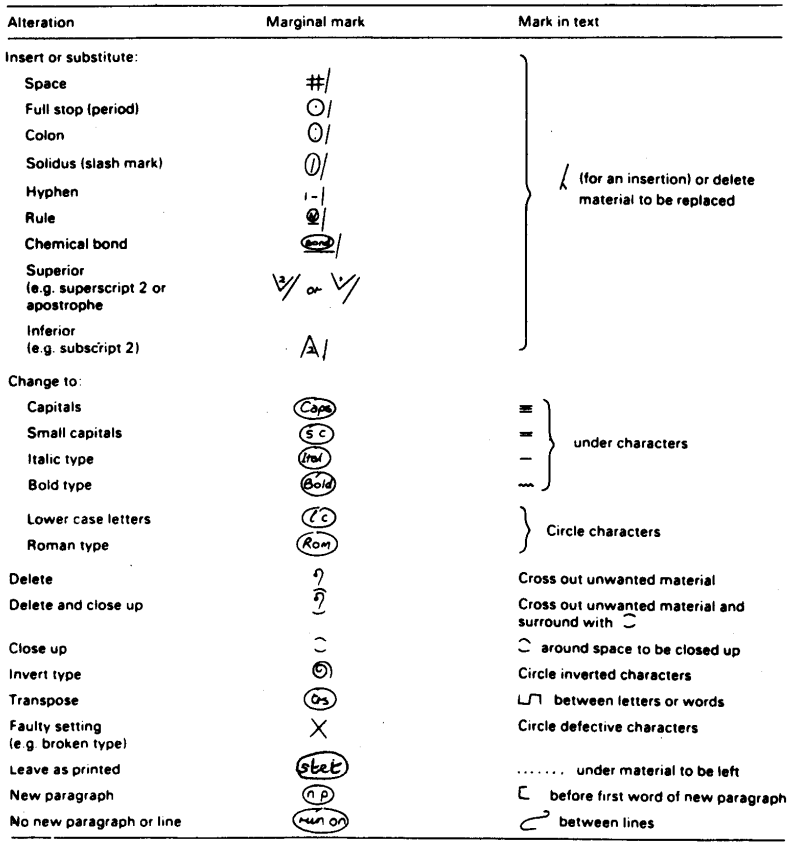

Alteration	Marginal mark	Mark in text
Insert or substitute:		/ (for an insertion) or delete material to be replaced
Space	#	
Full stop (period)	⊙	
Colon	⊙	
Solidus (slash mark)	⊙	
Hyphen	⊙	
Rule	⊙	
Chemical bond	bond	
Superior (e.g. superscript 2 or apostrophe	x^2 or x''	
Inferior (e.g. subscript 2)	A_2	
Change to:		
Capitals	caps	≡ under characters
Small capitals	sc	= under characters
Italic type	ital	– under characters
Bold type	bold	~ under characters
Lower case letters	lc	Circle characters
Roman type	rom	Circle characters
Delete	⊙	Cross out unwanted material
Delete and close up	⊙	Cross out unwanted material and surround with ⌒
Close up	⌒	⌒ around space to be closed up
Invert type	⊙	Circle inverted characters
Transpose	tr	⌴ between letters or words
Faulty setting (e.g. broken type)	X	Circle defective characters
Leave as printed	stet	..... under material to be left
New paragraph	n p	⊏ before first word of new paragraph
No new paragraph or line	run on	⁀ between lines

Please note
(a) No correction should be made in the text without an accompanying mark in the margin, or the correction may be easily missed.
(b) Complicated corrections can be explained in a covering letter.

Journal of
Applied Crystallography

ISSN 0021-8898

Editor: **Gernot Kostorz**

ORDER FORM
Return within 14 days of January 14 2005

YOU WILL AUTOMATICALLY BE SENT DETAILS OF HOW TO DOWNLOAD AN ELECTRONIC OFFPRINT OF YOUR PAPER, FREE OF CHARGE. PRINTED OFFPRINTS MAY BE PURCHASED USING THIS FORM.

Please keep a copy of this order and send the original to:

INTERNATIONAL UNION OF CRYSTALLOGRAPHY
5 Abbey Square
Chester CH1 2HU, England. Fax: +44 1244 314888

VAT No. GB 161 9034 76

Article No.: J050007-WF5009

Title of article	Perturbation method of analysis of crystal truncation rod data
Name	
Address	
E-mail address (for electronic offprints)	ikr@uiuc.edu

OPEN ACCESS

IUCr journals now offer authors the chance to make their articles open access on **Crystallography Journals Online**. For full details of our open access policy, see http://journals.iucr.org/services/openaccess.html.

The charge for making an article open access is **800 United States dollars**.

☐ I wish to make my article open access.

COLOUR OFFPRINTS

I wish to order . . . . . paid offprints

These offprints will be sent to the address given above. If the above address or e-mail address is not correct, please indicate an alternative:

PAYMENT

Charge for open access . . . . . USD Charge for offprints . . . . . USD Total charge . . . . . USD

☐ A cheque for . . . . . USD payable to **INTERNATIONAL UNION OF CRYSTALLOGRAPHY** is enclosed

☐ An official purchase order made out to **INTERNATIONAL UNION OF CRYSTALLOGRAPHY** ☐ is enclosed ☐ will follow

Purchase order No.

☐ Please invoice me

Date	Signature

OPEN ACCESS

The charge for making an article open access is **800 United States dollars**.

A paper may be made open access at any time after the proof stage on receipt of the appropriate payment. This includes all back articles on **Crystallography Journals Online**. For further details, please contact support@iucr.org. Likewise, organizations wishing to sponsor open-access publication of a series of articles or complete journal issues should contact support@iucr.org.

To check whether your organization has open-access membership, see http://scripts.iucr.org/cgi-bin/oa_inst_list

COLOUR OFFPRINTS

An electronic offprint is supplied free of charge.

Printed offprints without limit of number may be purchased at the prices given in the table below. The requirements of all joint authors, if any, and of their laboratories should be included in a single order, specifically ordered on the form overleaf. All orders for offprints must be submitted promptly; it will not be possible to supply offprints for orders received after the journal is printed.

Please note that normally offprints are sent about one month after publication of the article, and normally by surface mail. If offprints are wanted by air mail additional costs will be invoiced.

Prices for offprints are given below in **United States dollars** and include postage.

	Size of paper (in printed pages)				
Number of offprints required	1–2	3–4	5–8	9–16	Additional 8's
50	90	130	180	272	120
100	132	184	254	388	158
150	172	238	332	504	198
200	214	294	410	624	246
Additional 50's	42	54	78	118	40

Offprints with covers are only available by special order. Please contact the Managing Editor (at the address given below) for a quotation.

PAYMENT AND ORDERING

Cheques should be in **United States dollars** payable to **INTERNATIONAL UNION OF CRYSTALLOGRAPHY**. Official purchase orders should be made out to **INTERNATIONAL UNION OF CRYSTALLOGRAPHY**.

Orders should be returned by fax to:

INTERNATIONAL UNION OF CRYSTALLOGRAPHY
5 Abbey Square
Chester CH1 2HU, England. Fax: +44 1244 314888

ENQUIRIES

Enquiries concerning offprints should be sent to support@iucr.org.